Hindawi
International Journal of Aerospace Engineering
Volume 2023, Article ID 9980780, 16 pages
https://doi.org/10.1155/2023/9980780

Research Article

Integrated Dynamics of Space Rigid-Flex Combination System with Time-Varying Configuration

Yaen Xie,[1] **Xianliang Zhang**,[2] **Xiangshuai Song**,[1] **Xiaobin Lian**,[3] **and Jian Zhang**[3]

[1]*College of Aerospace and Civil Engineering, Harbin Engineering University, Harbin 150001, China*
[2]*School of Mathematics and Statistics, Taishan University, Taian 271021, China*
[3]*Shanghai Institute of Satellite Engineering, Shanghai 201109, China*

Correspondence should be addressed to Xianliang Zhang; xianliang_2013@163.com

Received 26 April 2023; Revised 15 June 2023; Accepted 25 August 2023; Published 13 September 2023

Academic Editor: Chuang Liu

Dual numbers were applied to the dynamics of a rigid-flexible combination system (RFCS) with time-varying configuration in this paper. The six-dimensional spinor form of the motion of flexible modules, including the dual vector, dual momentum, dual inertia operator, dual coupling coefficient operator, and dual-modal coordinates, was derived using the dual numbers that could represent spiral motion in a compact form. On this basis, the integrated dynamic model of a rigid-flexible combination system with a time-varying configuration was proposed. And then, the relative dynamics equations between two rigid-flexible combination systems which both have time-varying configuration were provided. An on-orbit assembly mission of flexible modules transported and operated by free-flying space robots (FFSRs) is presented as an exemplary application of relative dynamics. Simulation results illustrate the complex coupling effects on the relative motion between two rigid-flex combination systems with time-varying configuration.

1. Introduction

FFSRs present great potential for on-orbit assembly missions [1–6]. The implementation of in-space assembly using FFSR can be divided into three stages. The first step is module capture [7], which means that FFSR captures the module through the capture device; the module and FFSR constitute a combination system. The second step is module transportation [8]. The module is transported to the desired position and integrated through combination systems with large translational and rotational maneuvers. The last step is module docking [9]. The adjacent modules are ultimately connected together through docking mechanisms, achieving structural growth. In this paper, the dynamics of module transportation using FFSR are investigated.

Since the initial motion state of the module, including the attitude and position, is unknown during the capture process, one of the key mission requirements in the module transportation process is to adjust the postcapture configuration of the combination system. The aim of the above configuration adjustment is to prepare the best pose for assembly. Several dynamic modeling methods of the operation of free-floating rigid bodies have been proposed. Liu et al. [10] derived the capture and postcapture dynamics equations for the operation of a noncooperative space target by using FFSR. In this model, the influence of the contact force between the FFSR and the assembly module on the whole system motion was considered while catching a floating rigid body. Cyril and Chau et al. [11, 12] have investigated the dynamics for catching and operating a rigid body by assembly robots. In Refs. [13–16], the attitude dynamics of the combined systems consisting of a rigid service robot, a rigid target, and two rigid space manipulators were investigated. Li et al. [17] improved the attitude dynamics of the combined systems with flexible manipulators by considering the vibration influence on the motion of the whole system. The solutions obtained by the dynamics model mentioned above can handle a large number of motion description problems in space-capturing and postcapturing missions.

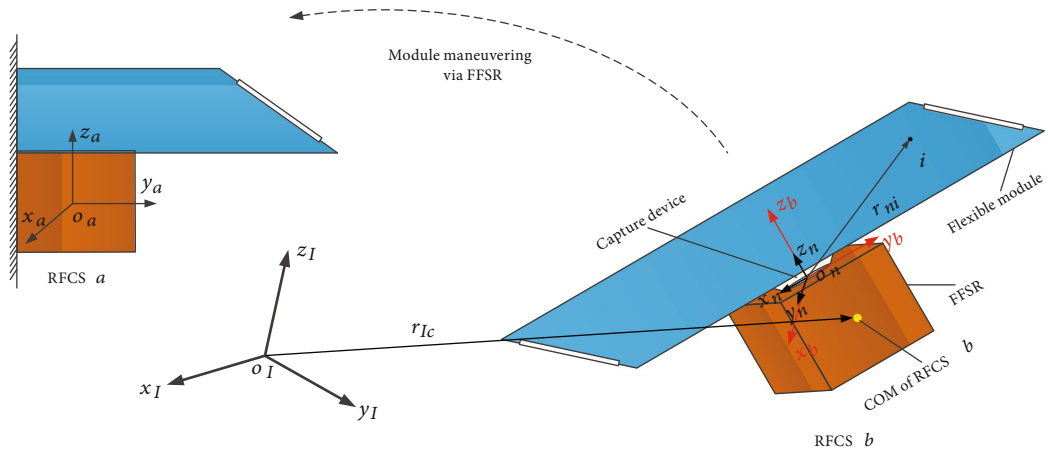

Figure 1: Mission system.

Another mission requirement of the module transportation process is to quickly transport the modules to the desired positions for integration by using FFSR. The foundation for meeting this requirement is to establish an accurate and engineering-applicable relative dynamics model for assembly robots. A lot of work has been done to describe the relative motion between two spacecrafts. The initial research on relative dynamics between two spacecrafts was investigated based on Newton's second law [18]. This relative equation was followed and improved upon by Clohessy and Wiltshire [19], who proposed the relative dynamics model in a simple form known as the C-W equations when the leader spacecraft is deployed in a circular orbit. Afterwards, Brodsky and Shoham [20] proposed a translation and rotation coupling dynamic model based on a dual quaternion. In the space station rendezvous and docking mission, the same integrated dynamic model was used to guide and control the spacecraft [21]. The above research on relative dynamics focuses on rigid bodies. Specifically, the object of capture and control is a rigid body, and the assembly robot is also a rigid body. However, in order to save mission time and improve robot work efficiency, in on-orbit assembly missions, structure modules are often designed with large dimensions and a light weight [22]. This design results in structural modules exhibiting flexible characteristics. The rigid-flexible coupling effect must be taken into consideration during module transportation by rigid FFSR. Sun et al. and Zhang et al. [23–25] proposed the relative dynamics between two rigid-flexible coupling spacecrafts for an in-space assembly mission, which considered both the engineering application advantages of rotating reference and the compactness representation advantages of dual numbers. The current achievements focus on the relative dynamic modeling of rigid bodies or RFCSs with stable configuration.

Generally speaking, these two actions, configuration adjustment and module transportation, can be carried out separately. However, in order to improve the efficiency of the on-orbit assembly mission, achieving the two actions at the same time is a better choice, that is, integrated motion. The equations proposed in this paper are to describe the complex coupling dynamics of this integrated motion based on dual quaternion. The main contributions of this paper are summarized as follows:

(a) The dual momentum and the dynamics model for RFCS with time-varying configuration were developed

(b) The relative dynamics equations between two RFCSs with time-varying configuration were proposed

The organizational structure of this paper is as follows. The application scenarios, coordinate systems, and modeling assumptions were introduced in Section 2. Section 3 developed the six-dimensional spinor of the flexible modules motion, and the dynamic model of RFCS with time-varying configuration was established. Then, in Section 4, the relative dynamics model between two RFCSs with time-varying configuration was established, and the coupling effect of the on-orbit assembly was analyzed. In Section 5, the simulation results of the integrated model proposed in this paper are presented. Finally, Section 6 provides the conclusion of this article.

2. Application Scenarios, Coordinate Systems, and Modeling Assumptions

The application mission scenario was designed to be flexible modules postcapture operation and transportation by rigid FFSRs to a preassembled configuration. As shown in Figure 1, the RFCS b consists of a flexible module and a FFSR; the flexible module and FFSR are connected by the capture device. In this paper, the capture device was assumed as a three-degree-of-freedom rotary pair; that is, the flexible module could perform a three-degree-of-freedom relative attitude motion relative to FFSR. In the on-orbit assembly mission, two actions were carried out at the same time for RFCS b, that is, configuration adjustment action and module transportation action. The configuration adjustment action is to prepare the best pose for assembly through the three-degree-of-freedom relative rotation between the flexible module and the FFSR. The module transportation action is to transport the flexible modules to the desired locations near RFCS a for integration. Figure 1 describes the in-space assembly mission

and the coordinate systems. The following four coordinate systems are used in this paper:

(a) Earth-centered inertial (ECI) coordinate system $o_I - x_I y_I z_I$. The $+z$ and $+x$ axes of the ECI coordinate system point at the north pole of the Earth and the vernal equinox, respectively. $+y$ axis completes the right-hand set

(b) Body-fixed (BF) coordinate system of RFCS a $o_a - x_a y_a z_a$. The origin of the BF coordinate system of RFCS a locates at the connection point between the module and FFSR. The $+x$ and $+z$ axes point at the relative measuring sensor and the module, respectively. $+y$ axis completes the right-hand set

(c) Body-fixed (BF) coordinate system of RFCS b $o_b - x_b y_b z_b$. The origin of the BF coordinate system of RFCS b locates at the connection point between the module and FFSR. The $+x$ and $+z$ axes point at the relative measuring sensor and the module, respectively. $+y$ axis completes the right-hand set

(d) Floating coordinate system of RFCS $bo_n - x_n y_n z_n$. The origin of $o_n - x_n y_n z_n$ coincides with the BF coordinate $o_b - x_b y_b z_b$, and at the initial moment, the three-axis coordinate direction of $o_n - x_n y_n z_n$ coincides with the BF coordinate system $o_b - x_b y_b z_b$. The difference is that the floating frame, $o_n - x_n y_n z_n$, is a flexible module follow-up coordinate system

In this paper, at the initial moment, the origin and three-axis coordinate direction of the BF coordinate system of RFCS b coincide with the floating frame of RFCS b. This construction of the coordinate system can simplify the calculation of the dual momentum of RFCS with a time-varying configuration. Detailed calculations can be found in Section 3.2.

The integrated dynamic model of a rigid-flex combination system with time-varying configuration based on dual quaternion was derived under the following assumption.

Assumption 1. Compared to the size of the module and FFSR, the vibration displacement of the module is a small amount.

3. Dynamics of RFCS with Time-Varying Configuration

A dual quaternion is a dual number with each element of the dual a quaternion, that is $\hat{q} = q + \varepsilon q'$, where q and q' are both quaternions. ε is the dual unit defined as $\varepsilon^2 = 0$ and $\varepsilon \neq 0$. The spacecraft dynamic model expressed in dual quaternion can be expressed in the same mathematical framework, which makes the representation of the relative dynamic model compact. This model is generally known as the integrated dynamic model. The compactness of representation is positively correlated with the computational efficiency of the relative dynamic model.

3.1. Motion of Flexible Module. The finite-element principle is a method of turning a continuous infinite degree-of-freedom problem into a discrete finite degree-of-freedom problem. A more specific discussion on the finite-element principle can be found in Refs. [26, 27]. According to the finite-element principle, the velocity of an arbitrary discrete element i of a flexible module relative to the COM of RFCS b can be expressed as

$$v_{i,c.m} = v_{b,c.m} + \omega_{b,c.m} \times r_{bn,c.m} + (\omega_{b,c.m} + \omega_{n,c.m}) \times (r_{ni,c.m} + u_{i,c.m}) + \dot{u}_{i,c.m}, \quad (1)$$

where $v_{i,c.m}$ is the velocity of i with respect to the COM of RFCS b. $v_{b,c.m}$ is the orbital velocity of the COM of RFCS b. $\omega_{b,c.m}$ is the angular velocity of RFCS b. $r_{bn,c.m}$ is the position vector from the COM of RFCS b to the origin of the BF coordinate system $o_b - x_b y_b z_b$. $\omega_{n,c.m}$ is the relative angular velocity between the flexible module and the FFSR. $r_{ni,c.m}$ denotes the position vector from the origin of the BF coordinate system $o_b - x_b y_b z_b$ to i. $u_{i,c.m}$ and $\dot{u}_{i,c.m}$ denote the elastic position and elastic velocity of i, respectively.

The dual velocity of the discrete element i with respect to the COM of RFCS b is

$$\hat{\omega}_{i,c.m} = \omega_{i,c.m} + \varepsilon v_{i,c.m}. \quad (2)$$

According to the algebra of dual numbers, the dual velocity of the discrete element i with respect to the origin of $o_b - x_b y_b z_b$, o_b, in terms of components along the BF coordinate system $o_b - x_b y_b z_b$ is

$$\hat{\omega}^b_{i,n} = \hat{R}_{nb,n} \hat{\omega}_{i,c.m}, \quad (3)$$

where

$$\hat{R}_{nb,n} = \left[1 + \varepsilon r^b_{nb,n}(\times)\right] = \begin{bmatrix} I_{3\times3} & 0_{3\times3} \\ \left[r^b_{nb,n}\right]^\times & I_{3\times3} \end{bmatrix}, \quad (4)$$

$r^b_{nb,n}$ is the position vector from the origin of the BF coordinate system $o_b - x_b y_b z_b$ to the COM of RFCS b in terms of components along the BF coordinate system $o_b - x_b y_b z_b$. $\left[r^b_{nb,n}\right]^\times$ denotes the cross-product matrix of $r^b_{nb,n}$. The cross-product matrix for an arbitrary third-order vector $x = [x_1 \quad x_2 \quad x_3]^T$ is

$$[x]^\times = \begin{bmatrix} 0 & -x_3 & x_2 \\ x_3 & 0 & -x_1 \\ -x_2 & x_1 & 0 \end{bmatrix}. \quad (5)$$

The dual momentum of i relative to the BF coordinate system $o_b - x_b y_b z_b$ is

$$\hat{H}^b_{i,n} = \hat{R}_{ni,n} \left[\hat{m}_i \left(\hat{R}_{nb,n} \hat{\omega}^b_{i,c.m}\right)\right], \quad (6)$$

where

$$\begin{aligned}\widehat{R}_{ni,n} &= \left\{1+\varepsilon\left[\left(r^b_{nb,n}+r^b_{bi,n}+u^b_{i,n}\right)\times\right]\right\}\\ &= \left\{1+\varepsilon\left[\left(r^b_{nb,n}+r^b_{bn,n}+r^b_{ni,n}+u^b_{i,n}\right)\times\right]\right\}\\ &= \left\{1+\varepsilon\left[\left(r^b_{ni,n}+u^b_{i,n}\right)\times\right]\right\}\end{aligned} \tag{7}$$

and $r^b_{bn,n}$, $r^b_{ni,n}$, and $u^b_{i,n}$ denote the vectors $r_{bn,n}$, $r_{ni,n}$, and $u_{i,n}$ represented relative to the BF coordinate system $o_b - x_b y_b z_b$, and $r^b_{bn,n} \equiv r^b_{bn,c.m}$, $r^b_{ni,n} \equiv r^b_{ni,c.m}$, and $u^b_{i,n} \equiv u^b_{i,c.m}$.

Substituting Equation (7) into Equation (6). According to Assumption 1, $\|u^b_i\| << r^b_{ni,n}$ and $\|u^b_i\| << r^b_{nb,n}$. Therefore, the elastic displacement u^b_i can be neglected in the calculation of Equation (6). Subsequently, Equation (6) can be further expressed as

$$\begin{aligned}\widehat{H}^b_{i,n} &= \left\{1+\varepsilon\left[\left(r^b_{ni,n}+u^b_{i,n}\right)\times\right]\right\}\left[\widehat{m}_i\left(\widehat{R}_{nb,n}\widehat{\omega}^b_{i,c.m}\right)\right]\\ &= \left[1+\varepsilon\left(r^b_{ni,n}+u^b_{i,n}\right)^\times\right]\left[m_i\left(v^b_{i,c.m}+r^b_{nb,n}\times\omega^b_{i,c.m}\right)\right]\\ &= m_i v^b_{i,c.m}+m_i\left[r^b_{nb,n}\right]^\times\omega^b_{i,c.m}\\ &\quad+\varepsilon\left[r^b_{ni,n}\times\left(m_i v^b_{i,c.m}+m_i\left[r^b_{nb,n}\right]^\times\omega^b_{i,c.m}\right)\right]\\ &= m_i v^b_{i,c.m}+m_i\left[r^b_{nb,n}\right]^\times\omega^b_{i,c.m}\\ &\quad+\varepsilon\left(m_i\left[r^b_{ni,n}\right]^\times v^b_{i,c.m}+m_i\left[r^b_{ni,n}\right]^\times\left[r^b_{nb,n}\right]^\times\omega^b_{i,c.m}\right).\end{aligned} \tag{8}$$

Substituting Equation (1) and Equation (2) into Equation (8), the dual momentum of i can be further expressed as

$$\begin{aligned}\widehat{H}^b_{i,n} &= m_i v^b_{i,c.m}+m_i\left[r^b_{nb,n}\right]^\times\omega^b_{i,c.m}\\ &\quad+\varepsilon\left(m_i\left[r^b_{ni,n}\right]^\times v^b_{i,c.m}+m_i\left[r^b_{ni,n}\right]^\times\left[r^b_{nb,n}\right]^\times\omega^b_{i,c.m}\right)\\ &= m_i v^b_{b,c.m}+m_i\left[r^b_{bn,c.m}\right]^\times_V\omega^b_{b,c.m}\\ &\quad+m_i\left[r^b_{ni,c.m}\right]^\times_V\left(\omega^b_{b,c.m}+\omega^b_{n,c.m}\right)\\ &\quad+m_i\dot{u}^b_{i,c.m}+m_i\left[r^b_{nb,n}\right]^\times\omega^b_{i,c.m}+\varepsilon m_i\left[r^b_{ni,n}\right]^\times v^b_{b,c.m}\\ &\quad+\varepsilon m_i\left[r^b_{ni,n}\right]^\times\left[r^b_{bn,c.m}\right]^\times_V\omega^b_{b,c.m}+\varepsilon m_i\left[r^b_{ni,n}\right]^\times\left[r^b_{ni,c.m}\right]^\times_V\\ &\quad\cdot\left(\omega^b_{b,c.m}+\omega^b_{n,c.m}\right)+\varepsilon m_i\left[r^b_{ni,n}\right]^\times\dot{u}^b_{i,c.m}\\ &\quad+m_i\left[r^b_{ni,n}\right]^\times\left[r^b_{nb,n}\right]^\times\left(\omega^b_{b,c.m}+\omega^b_{n,c.m}\right).\end{aligned} \tag{9}$$

In Equation (9), the following operational relationship holds

$$\left[r^b_{nb,n}\right]^\times = -\left[r^b_{bn,n}\right]^\times, \tag{10}$$

$$m_i\left[r^b_{ni,c.m}\right]^\times_V\omega^b_{b,c.m} = -m_i\left[r^b_{ni,c.m}\right]^\times\omega^b_{b,c.m}, \tag{11}$$

$$m_i\left[r^b_{ni,c.m}\right]^\times_V\omega^b_{n,c.m} = -m_i\left[r^b_{ni,c.m}\right]^\times\omega^b_{n,c.m}, \tag{12}$$

where $[r^b_{ni,c.m}]^\times_V\omega^b_{n,c.m} = [\omega^b_{n,c.m}]^\times r^b_{ni,c.m}$.

According to Equations (10), (11), and (12), Equation (9) can be expressed in an explicit form

$$\begin{aligned}\widehat{H}^b_{i,n} &= m_i v^b_{i,c.m}+m_i\left[r^b_{nb,n}\right]^\times\omega^b_{i,c.m}\\ &\quad+\varepsilon\left(m_i\left[r^b_{ni,n}\right]^\times v^b_{i,c.m}+m_i\left[r^b_{ni,n}\right]^\times\left[r^b_{nb,n}\right]^\times\omega^b_{i,c.m}\right)\\ &= m_i v^b_{b,c.m}+m_i\left[r^b_{nb,c.m}\right]^\times\omega^b_{b,c.m}-m_i\left[r^b_{ni,c.m}\right]^\times\\ &\quad\cdot\left(\omega^b_{b,c.m}+\omega^b_{n,c.m}\right)+m_i\dot{u}^b_{i,c.m}+m_i\left[r^b_{nb,n}\right]^\times\left(\omega^b_{b,c.m}+\omega^b_{n,c.m}\right)\\ &\quad+\varepsilon m_i\left[r^b_{ni,n}\right]^\times v^b_{b,c.m}+\varepsilon m_i\left[r^b_{ni,n}\right]^\times\left[r^b_{nb,c.m}\right]^\times\omega^b_{b,c.m}\\ &\quad-\varepsilon m_i\left[r^b_{ni,n}\right]^\times\left[r^b_{ni,c.m}\right]^\times\left(\omega^b_{b,c.m}+\omega^b_{n,c.m}\right)+\varepsilon m_i\left[r^b_{ni,n}\right]^\times\dot{u}^b_{i,c.m}\\ &\quad+\varepsilon m_i\left[r^b_{ni,n}\right]^\times\left[r^b_{nb,n}\right]^\times\left(\omega^b_{b,c.m}+\omega^b_{n,c.m}\right)\\ &= m_i v^b_{b,c.m}+m_i\left[r^b_{bi,c.m}\right]^\times\omega^b_{b,c.m}+m_i\left[r^b_{bi,c.m}\right]^\times\omega^b_{n,c.m}\\ &\quad+m_i\left[r^b_{nb,n}\right]^\times\omega^b_{b,c.m}+m_i\dot{u}^b_{i,c.m}+\varepsilon m_i\left[r^b_{ni,n}\right]^\times v^b_{b,c.m}\\ &\quad+\varepsilon m_i\left[r^b_{ni,n}\right]^\times\left[r^b_{bi,c.m}\right]^\times\omega^b_{b,c.m}+\varepsilon m_i\left[r^b_{ni,n}\right]^\times\left[r^b_{bi,c.m}\right]^\times\omega^b_{n,c.m}\\ &\quad+\varepsilon m_i\left[r^b_{ni,n}\right]^\times\left[r^b_{nb,n}\right]^\times\omega^b_{b,c.m}+\varepsilon m_i\left[r^b_{ni,n}\right]^\times\dot{u}^b_{i,c.m}.\end{aligned} \tag{13}$$

In Equation (13), $r^b_{bi,c.m} \triangleq r^b_{bi,n}$, and the following operational relationship holds

$$\varepsilon m_i\left[r^b_{ni,n}\right]^\times v^b_{b,c.m} = \varepsilon m_i\left[r^b_{nb,n}\right]^\times v^b_{b,c.m}+\varepsilon m_i\left[r^b_{bi,n}\right]^\times v^b_{b,c.m}, \tag{14}$$

$$\begin{aligned}\varepsilon m_i\left[r^b_{ni,n}\right]^\times\left[r^b_{bi,c.m}\right]^\times\omega^b_{b,c.m} &= \varepsilon m_i\left[r^b_{nb,n}\right]^\times\left[r^b_{bi,c.m}\right]^\times\omega^b_{b,c.m}\\ &\quad+\varepsilon m_i\left[r^b_{bi,n}\right]^\times\left[r^b_{bi,c.m}\right]^\times\omega^b_{b,c.m},\end{aligned} \tag{15}$$

$$\begin{aligned}\varepsilon m_i\left[r^b_{ni,n}\right]^\times\left[r^b_{nb,n}\right]^\times\omega^b_{b,c.m} &= \varepsilon m_i\left[r^b_{nb,n}\right]^\times\left[r^b_{nb,n}\right]^\times\omega^b_{b,c.m}\\ &\quad+\varepsilon m_i\left[r^b_{bi,n}\right]^\times\left[r^b_{nb,n}\right]^\times\omega^b_{b,c.m},\end{aligned} \tag{16}$$

$$\varepsilon m_i\left[r^b_{ni,n}\right]^\times\dot{u}^b_{i,c.m} = \varepsilon m_i\left[r^b_{nb,n}\right]^\times\dot{u}^b_{i,c.m}+\varepsilon m_i\left[r^b_{bi,n}\right]^\times\dot{u}^b_{i,c.m}. \tag{17}$$

According to the finite-element principle, the dual momentum of the flexible module with respect to the BF coordinate system $o_b - x_b y_b z_b$ can be expressed as

$$\widehat{H}_{fl,n}^{b} = \sum_{i=1}^{n} \widehat{H}_{i,n}^{b}. \tag{18}$$

Substituting Equations (13), (14), (15), (16), and (17) into Equation (18), the dual momentum of the flexible module can be obtained.

$$\begin{aligned}\widehat{H}_{fl,n}^{b} = {} & \sum_{i=1}^{n} m_i v_{b,c.m}^{b} + \sum_{i=1}^{n} m_i \left[r_{bi,c.m}^{b}\right]^{\times} \omega_{b,c.m}^{b} + \sum_{i=1}^{n} m_i \left[r_{bi,c.m}^{b}\right]^{\times} \omega_{n,c.m}^{b} \\ & + \sum_{i=1}^{n} m_i \left[r_{nb,n}^{b}\right]^{\times} \omega_{b,c.m}^{b} + \sum_{i=1}^{n} m_i \dot{u}_{i,c.m}^{b} + \varepsilon \sum_{i=1}^{n} m_i \left[r_{nb,n}^{b}\right]^{\times} v_{b,c.m}^{b} \\ & + \varepsilon \sum_{i=1}^{n} m_i \left[r_{bi,n}^{b}\right]^{\times} v_{b,c.m}^{b} + \varepsilon \sum_{i=1}^{n} m_i \left[r_{nb,n}^{b}\right]^{\times} \left[r_{bi,c.m}^{b}\right]^{\times} \omega_{b,c.m}^{b} \\ & + \varepsilon \sum_{i=1}^{n} m_i \left[r_{bi,n}^{b}\right]^{\times} \left[r_{bi,c.m}^{b}\right]^{\times} \omega_{b,c.m}^{b} + \varepsilon \sum_{i=1}^{n} m_i \left[r_{nb,n}^{b}\right]^{\times} \left[r_{bi,c.m}^{b}\right]^{\times} \omega_{n,c.m}^{b} \\ & + \varepsilon \sum_{i=1}^{n} m_i \left[r_{bi,n}^{b}\right]^{\times} \left[r_{bi,c.m}^{b}\right]^{\times} \omega_{n,c.m}^{b} + \varepsilon \sum_{i=1}^{n} m_i \left[r_{ni,n}^{b}\right]^{\times} \left[r_{nb,n}^{b}\right]^{\times} \omega_{b,c.m}^{b} \\ & + \varepsilon \sum_{i=1}^{n} m_i \left[r_{ni,n}^{b}\right]^{\times} \dot{u}_{i,c.m}^{b}. \end{aligned} \tag{19}$$

In addition, let

$$\begin{aligned} \left[V_{fl}\right]^{\times} &= \sum_{i=1}^{n} m_i \left[r_{bi,n}^{b}\right]^{\times}, \left[V_{fl}\right]_{v}^{\times} = \sum_{i=1}^{n} m_i \left[r_{bi,n}^{b}\right]_{v}^{\times}, \\ m_{fl} &= \sum_{i=1}^{n} m_i, J_{fl} = \sum_{i=1}^{n} m_i \left[r_{bi,n}^{b}\right]^{\times} \left[r_{bi,n}^{b}\right]_{v}^{\times}, \end{aligned} \tag{20}$$

where J_{fl} denotes the moment of inertia of the flexible module. m_{fl} is the mass of the flexible module.

Having derived the discrete equation of the dual momentum, we perform the following model transformation on Equation (19).

$$\begin{aligned} u_i^b &= \Phi_i \eta, \\ \dot{u}_i^b &= \Phi_i \dot{\eta}. \end{aligned} \tag{21}$$

As shown in Equation (21), the module vibration displacement can have a linear equation relationship with the modal coordinates, η, through the matrix of eigenvectors of i, Φ_i. $\dot{\eta}$ is the first derivative of η.

According to Ref. [28], the following equation transformations can be obtained.

$$\begin{aligned} B_{\text{tran}} &= \sum_{i=1}^{n} m_i \Phi_i, \\ B_{\text{rot}} &= \sum_{i=1}^{n} m_i \left[r_{ci}^{b}\right]^{\times} \Phi_i, \end{aligned} \tag{22}$$

where B_{tran} and B_{rot} are the rigid-flex translational and rotational coupling matrices, respectively. Substituting Equations (20), (21), and (22) into Equation (19), the dual momentum of the flexible module in hybrid coordinate can be expressed as

$$\begin{aligned}\widehat{H}_{fl,n}^{b} = {} & m_{fl} v_{b,c.m}^{b} + r_{nb,n}^{\times} m_{fl} \omega_{b,c.m}^{b} + \left[V_{fl}\right]_{v}^{\times} \omega_{b,c.m}^{b} \\ & + \left[V_{fl}\right]^{\times} \omega_{n,c.m}^{b} + B_{\text{tran}} \dot{\eta} + \varepsilon r_{nb,n}^{\times} \left[V_{fl}\right]_{v}^{\times} \omega_{b,c.m}^{b} \\ & + \varepsilon J_{fl} \omega_{b,c.m}^{b} + \varepsilon r_{nb,n}^{\times} r_{nb,n}^{\times} m_{fl} \omega_{b,c.m}^{b} + \varepsilon r_{nb,n}^{\times} m_{fl} v_{b,c.m}^{b} \\ & + \varepsilon r_{nb,n}^{\times} \left[V_{fl}\right]^{\times} \omega_{b,c.m}^{b} + \varepsilon \left[V_{fl}\right]^{\times} v_{b,c.m}^{b} + \varepsilon r_{nb,n}^{\times} \left[V_{fl}\right]^{\times} \omega_{n,c.m}^{b} \\ & + \varepsilon J_{fl} \omega_{n,c.m}^{b} + \varepsilon r_{nb,n}^{\times} B_{\text{tran}} \dot{\eta} + \varepsilon B_{\text{rot}} \dot{\eta}. \end{aligned} \tag{23}$$

Representing Equation (16) in six-dimensional spinor form

$$\begin{aligned}\widehat{H}_{fl,n}^{b} = {} & \begin{bmatrix} I_{3\times3} & 0 \\ r_{nb,n}^{\times} & I_{3\times3} \end{bmatrix} \begin{bmatrix} \left[V_{fl}\right]_{v}^{\times} & m_{fl} I_{3\times3} \\ J_{fl} & \left[V_{fl}\right]^{\times} \end{bmatrix} \\ & \cdot \left(\begin{bmatrix} I_{3\times3} & 0 \\ r_{nb,n}^{\times} & I_{3\times3} \end{bmatrix} \begin{bmatrix} \omega_{b,c.m}^{b} \\ v_{b,c.m}^{b} \end{bmatrix} \right) \\ & + \begin{bmatrix} I_{3\times3} & 0 \\ r_{nb,n}^{\times} & I_{3\times3} \end{bmatrix} \begin{bmatrix} \left[V_{fl}\right]^{\times} \\ J_{fl} \end{bmatrix} \omega_{n,c.m}^{b} \\ & + \begin{bmatrix} I_{3\times3} & 0 \\ r_{nb,n}^{\times} & I_{3\times3} \end{bmatrix} \begin{bmatrix} B_{\text{tran}} & 0 \\ 0 & B_{\text{rot}} \end{bmatrix} \begin{bmatrix} \dot{\eta} \\ \dot{\eta} \end{bmatrix}. \end{aligned} \tag{24}$$

By symbolizing Equation (24), we obtain

$$\widehat{H}_{fl,n}^{b} = \widehat{R}_{nb,n} \widehat{M}_{fl} \left(\widehat{\omega}_{n,c.m}^{b} + \widehat{R}_{nb,n} \widehat{\omega}_{b,c.m}^{b} \right) + \widehat{R}_{nb,n} \widehat{B}_{cp} \dot{\widehat{\eta}}, \tag{25}$$

where $\widehat{\omega}_{n,c.m}^{b} = \begin{bmatrix} \omega_{n,c.m}^{b} \\ 0 \end{bmatrix} \in \mathbb{R}^{6\times1}$ is the dual velocity of the flexible module relative to FFSR. The dual inertia matrix $\widehat{M}_{fl} = \begin{bmatrix} \left[V_{fl}\right]_{v}^{\times} & m_{fl} I_{3\times3} \\ J_{fl} & \left[V_{fl}\right]^{\times} \end{bmatrix} \in \mathbb{R}^{6\times6}$ is a six-dimensional parameter matrix. The dual velocity $\widehat{\omega}_{b,c.m}^{b} = \begin{bmatrix} \omega_{b,c.m}^{b} \\ v_{b,c.m}^{b} \end{bmatrix} \in \mathbb{R}^{6\times1}$ is presented in terms of components along the BF coordinate system. $\widehat{B}_{cp} = \begin{bmatrix} B_{\text{tran}} & 0_{3\times N} \\ 0_{3\times N} & B_{\text{rot}} \end{bmatrix} \in \mathbb{R}^{6\times2N}$ is a new parameter for the dual representation of a rigid-flex combination system, which is defined as the rigid-flex dual coupling matrix. $\widehat{\eta} = \begin{bmatrix} \eta \\ \eta \end{bmatrix} \in \mathbb{R}^{2N\times1}$ is also a new parameter for the dual representation of a rigid-flex combination system, which is defined as the dual-modal coordinates.

Taking the first derivative of Equation (25), we obtain

$$\begin{aligned}\frac{d\widehat{H}^b_{fl,n}}{dt} &= \frac{\partial \widehat{H}^b_{fl,n}}{\partial t} + \left(\widehat{\omega}^b_{n,c.m} + \widehat{R}_{nb,n}\widehat{\omega}^b_{b,c.m}\right) \times \widehat{H}^b_{fl,n} \\ &= \widehat{R}_{nb,n}\widehat{M}_{fl}\left(\dot{\widehat{\omega}}^b_{n,c.m} + \widehat{R}_{nb,n}\dot{\widehat{\omega}}^b_{b,c.m}\right) + \widehat{R}_{nb,n}\widehat{B}_{cp}\ddot{\widehat{\eta}} \\ &\quad + \left(\widehat{\omega}^b_{n,c.m} + \widehat{R}_{nb,n}\widehat{\omega}^b_{b,c.m}\right) \\ &\quad \times \left[\widehat{R}_{nb,n}\widehat{M}_{fl}\left(\widehat{\omega}^b_{n,c.m} + \widehat{R}_{nb,n}\widehat{\omega}^b_{b,c.m}\right) + \widehat{R}_{nb,n}\widehat{B}_{cp}\dot{\widehat{\eta}}\right],\end{aligned} \tag{26}$$

Equation (26) can be further expressed as

$$\begin{aligned}\frac{d\widehat{H}^b_{fl,n}}{dt} &= \widehat{R}_{nb,n}\widehat{M}_{fl}\left(\widehat{R}_{nb,n}\dot{\widehat{\omega}}^b_{b,c.m}\right) + \widehat{R}_{nb,n}\widehat{\omega}^b_{b,c.m} \\ &\quad \times \left(\widehat{R}_{nb,n}\widehat{M}_{fl}\left(\widehat{R}_{nb,n}\widehat{\omega}^b_{b,c.m}\right)\right) + \widehat{R}_{nb,n}\widehat{M}_{fl}\dot{\widehat{\omega}}^b_{n,c.m} + \widehat{R}_{nb,n}\widehat{\omega}^b_{b,c.m} \\ &\quad \times \left(\widehat{R}_{nb,n}\widehat{M}_{fl}\widehat{\omega}^b_{n,c.m}\right) + \widehat{R}_{nb,n}\widehat{\omega}^b_{b,c.m} \times \widehat{R}_{nb,n}\widehat{B}_{cp}\dot{\widehat{\eta}} + \widehat{\omega}^b_{n,c.m} \\ &\quad \times \left[\widehat{R}_{nb,n}\widehat{M}_{fl}\left(\widehat{\omega}^b_{n,c.m} + \widehat{R}_{nb,n}\widehat{\omega}^b_{b,c.m}\right) + \widehat{R}_{nb,n}\widehat{B}_{cp}\dot{\widehat{\eta}}\right] + \widehat{R}_{nb,n}\widehat{B}_{cp}\ddot{\widehat{\eta}}.\end{aligned} \tag{27}$$

In addition, let

$$\begin{aligned}\widehat{F}^b_{DR,n} &= \widehat{R}_{nb,n}\widehat{M}_{fl}\dot{\widehat{\omega}}^b_{n,c.m} + \widehat{R}_{nb,n}\widehat{B}_{cp}\ddot{\widehat{\eta}} + \widehat{\omega}^b_{n,c.m} \\ &\quad \times \widehat{R}_{nb,n}\widehat{M}_{fl}\left(\widehat{R}_{nb,n}\widehat{\omega}^b_{b,c.m}\right) + \left(\widehat{\omega}^b_{n,c.m} + \widehat{R}_{nb,n}\widehat{\omega}^b_{b,c.m}\right) \\ &\quad \times \left(\widehat{R}_{nb,n}\widehat{M}_{fl}\widehat{\omega}^b_{n,c.m} + \widehat{R}_{nb,n}\widehat{B}_{cp}\dot{\widehat{\eta}}\right) = \widehat{R}_{nb,n}\widehat{M}_{fl}\dot{\widehat{\omega}}^b_{n,c.m} \\ &\quad + \widehat{R}_{nb,n}\widehat{B}_{cp}\ddot{\widehat{\eta}} + \widehat{\omega}^b_{n,c.m} \times \widehat{R}_{nb,n}\widehat{M}_{fl}\widehat{\omega}^b_{n,c.m} \\ &\quad + \left(\widehat{\omega}^b_{n,c.m} + \widehat{R}_{nb,n}\widehat{\omega}^b_{b,c.m}\right) \times \widehat{R}_{nb,n}\widehat{B}_{cp}\dot{\widehat{\eta}},\end{aligned} \tag{28}$$

where $\widehat{F}^b_{DR,n}$ is the force between the FFSR and the flexible module. $\widehat{F}^b_{DR,n} = \widehat{F}^b_{DE,n} + \widehat{F}^b_{CN,n}$ contains two parts, one is the driving force of FFSR acting on the flexible module, $\widehat{F}^b_{DE,n}$, and the other is the connection force between FFSR and the flexible module, $\widehat{F}^b_{CN,n}$.

3.2. Dual Number Representation of FFSR Motion. FFSR is the rigid part of RFCS b, assuming j is a nominal point of FFSR. The velocity of j can be represented as

$$v_{j,c.m} = v_{b,c.m} + \omega_{b,c.m} \times r_{bj,c.m}. \tag{29}$$

Note that $v_{j,c.m}$ is obtained relative to the COM of RFCS b.

Furthermore, we can obtain the dual velocity of the particle j.

$$\widehat{\omega}_{j,c.m} = \omega_{j,c.m} + \varepsilon v_{j,c.m}, \tag{30}$$

where $\omega_{j,c.m} \equiv \omega_{b,c.m}$. Similarly, $\widehat{\omega}_{j,c.m}$ is presented relative to the COM of RFCS b.

Then, according to the operation rules of dual quaternion, the dual velocity j relative to the origin of the BF coordinate system is obtained.

$$\widehat{\omega}^b_{j,.n} = \widehat{R}_{nb,n}\widehat{\omega}_{j,c.m}. \tag{31}$$

Note that $\widehat{\omega}^b_{j,.n}$ is a dual vector in terms of components along the BF coordinate system.

Based on the dual velocity of j, we can further obtain the dual momentum of j.

$$\widehat{H}^b_{j,n} = \widehat{R}_{nj,n}\left[\widehat{m}_j\left(\widehat{R}_{nb,n}\widehat{\omega}^b_{j,c.m}\right)\right]. \tag{32}$$

Substituting Equation (32) into Equation (31), we perform specific operations on the dual momentum of j and obtain

$$\begin{aligned}\widehat{H}^b_{j,n} &= \widehat{R}_{nj,n}\left[\widehat{m}_j\left(\widehat{R}_{nb,n}\widehat{\omega}^b_{j,c.m}\right)\right] \\ &= m_j v^b_{b,c.m} + m_j\left[r^b_{bj,n}\right]^\times_V \omega^b_{b,c.m} + m_j\left[r^b_{nb,n}\right]^\times \omega^b_{b,c.m} \\ &\quad + \varepsilon m_j\left[r^b_{nb,n}\right]^\times v^b_{b,n} + \varepsilon m_j\left[r^b_{nb,n}\right]^\times\left[r^b_{bj,n}\right]^\times_V \omega^b_{b,c.m} \\ &\quad + \varepsilon m_j\left[r^b_{nb,n}\right]^\times\left[r^b_{nb,n}\right]^\times \omega^b_{b,c.m} + \varepsilon m_j\left[r^b_{bj,n}\right]^\times v^b_{b,c.m} \\ &\quad + \varepsilon m_j\left[r^b_{bj,n}\right]^\times\left[r^b_{bj,n}\right]^\times_V \omega^b_{b,c.m} + \varepsilon m_j\left[r^b_{bj,n}\right]^\times\left[r^b_{nb,n}\right]^\times \omega^b_{b,c.m}.\end{aligned} \tag{33}$$

By simplifying Equation (33), one can obtain

$$\begin{aligned}\widehat{H}^b_{fr,n} &= \sum_{j=1}^{m}\widehat{H}^b_{j,n} = m_{fr}v^b_{b,c.m} + \left[V_{fr}\right]^\times_v \omega^b_{b,c.m} \\ &\quad + m_{fr}\left[r^b_{nb,n}\right]^\times \omega^b_{b,c.m} + \varepsilon\left[V_{fr}\right]^\times v^b_{b,c.m} + \varepsilon J_{fr}\omega^b_{b,c.m} \\ &\quad + \varepsilon m_{fr}\left[r^b_{nb,n}\right]^\times v^b_{b,c.m} + \varepsilon\left[V_{fr}\right]^\times_v\left[r^b_{nb,n}\right]^\times \omega^b_{b,c.m} \\ &\quad + \varepsilon m_{fr}\left[r^b_{nb,n}\right]^\times\left[r^b_{nb,n}\right]^\times \omega^b_{b,c.m} + \varepsilon\left[V_{fr}\right]^\times\left[r^b_{nb,n}\right]^\times \omega^b_{b,c.m},\end{aligned} \tag{34}$$

where

$$\begin{aligned}\left[V_{fr}\right]^\times &= \sum_{j=1}^{n} m_j\left[r^b_{bj,n}\right]^\times, \left[V_{fr}\right]^\times_v = \sum_{j=1}^{n} m_j\left[r^b_{bj,n}\right]^\times_v, \\ m_{fr} &= \sum_{j=1}^{n} m_j, J_{fr} = \sum_{j=1}^{n} m_j\left[r^b_{bj,n}\right]^\times\left[r^b_{bj,n}\right]^\times_v.\end{aligned} \tag{35}$$

J_{fr} is the moment of inertia of FFSR. m_{fr} is the mass of FFSR.

Representing Equation (16) in six-dimensional spinor form, one can obtain

$$\widehat{H}_{fr,n}^{b}=\begin{bmatrix} I_{3\times3} & 0_{3\times3} \\ r_{nb,n}^{\times} & I_{3\times3} \end{bmatrix}\begin{bmatrix} [V_{fr}]_{v}^{\times} & m_{fr}I_{3\times3} \\ J_{fr} & [V_{fr}]^{\times} \end{bmatrix}\left(\begin{bmatrix} I_{3\times3} & 0_{3\times3} \\ r_{nb,n}^{\times} & I_{3\times3} \end{bmatrix}\begin{bmatrix} \omega_{b,c.m}^{b} \\ v_{b,c.m}^{b} \end{bmatrix}\right). \tag{36}$$

By symbolizing Equation (24), we obtain

$$\widehat{H}_{fr,n}^{b}=\widehat{R}_{nb,n}\widehat{M}_{fr}\left(\widehat{R}_{nb,n}\widehat{\omega}_{b,c.m}^{b}\right), \tag{37}$$

where $\widehat{M}_{fr}=\begin{bmatrix} [V_{fr}]_{v}^{\times} & m_{fr}I_{3\times3} \\ J_{fr} & [V_{fr}]^{\times} \end{bmatrix}\in\mathbb{R}^{6\times6}$ is the dual inertia operator of FFSR.

Taking the first derivative of Equation (37), one can obtain

$$\begin{aligned}\frac{d\widehat{H}_{fr,n}^{b}}{dt}&=\frac{\partial\widehat{H}_{fr,n}^{b}}{\partial t}+\left(\widehat{R}_{nb,n}\widehat{\omega}_{b,c.m}^{b}\right)\times\widehat{H}_{fr,n}^{b}\\&=\widehat{R}_{nb,n}\widehat{M}_{fr}\left(\widehat{R}_{nb,n}\dot{\widehat{\omega}}_{b,c.m}^{b}\right)+\left(\widehat{R}_{nb,n}\widehat{\omega}_{b,c.m}^{b}\right)\\&\quad\times\widehat{R}_{nb,n}\widehat{M}_{fr}\left(\widehat{R}_{nb,n}\widehat{\omega}_{b,c.m}^{b}\right).\end{aligned} \tag{38}$$

3.3. Dynamics Modeling of RFCS b with Time-Varying Configuration. The dual momentum of RFCS b is the sum of the dual momentum of the flexible module and rigid FFSR.

$$\begin{aligned}\widehat{F}_{b,n}^{b}&=\frac{d\widehat{H}_{fr,n}^{b}}{dt}+\frac{d\widehat{H}_{fl,n}^{b}}{dt}=\widehat{R}_{nb,n}\widehat{M}_{fr}\left(\widehat{R}_{nb,n}\dot{\widehat{\omega}}_{b,c.m}^{b}\right)+\left(\widehat{R}_{nb,n}\widehat{\omega}_{b,c.m}^{b}\right)\\&\quad\times\widehat{R}_{nb,n}\widehat{M}_{fr}\left(\widehat{R}_{nb,n}\widehat{\omega}_{b,c.m}^{b}\right)+\widehat{R}_{nb,n}\widehat{M}_{fl}\left(\dot{\widehat{\omega}}_{n,c.m}^{b}+\widehat{R}_{nb,n}\dot{\widehat{\omega}}_{b,c.m}^{b}\right)\\&\quad+\widehat{R}_{nb,n}\widehat{B}_{cp}\ddot{\widehat{\eta}}+\left(\widehat{\omega}_{n,c.m}^{b}+\widehat{R}_{nb,n}\widehat{\omega}_{b,c.m}^{b}\right)\\&\quad\times\left[\widehat{R}_{nb,n}\widehat{M}_{fl}\left(\widehat{\omega}_{n,c.m}^{b}+\widehat{R}_{nb,n}\widehat{\omega}_{b,c.m}^{b}\right)+\widehat{R}_{nb,n}\widehat{B}_{cp}\dot{\widehat{\eta}}\right].\end{aligned} \tag{39}$$

Equation (39) can be further expressed as

$$\begin{aligned}\widehat{F}_{b,n}^{b}&=\widehat{R}_{nb,n}\left(\widehat{M}_{fr}+\widehat{M}_{fl}\right)\left(\widehat{R}_{nb,n}\dot{\widehat{\omega}}_{b,c.m}^{b}\right)+\left(\widehat{R}_{nb,n}\widehat{\omega}_{b,c.m}^{b}\right)\\&\quad\times\widehat{R}_{nb,n}\left(\widehat{M}_{fr}+\widehat{M}_{fl}\right)\left(\widehat{R}_{nb,n}\widehat{\omega}_{b,c.m}^{b}\right)+\widehat{R}_{nb,n}\widehat{M}_{fl}\dot{\widehat{\omega}}_{n,c.m}^{b}\\&\quad+\widehat{R}_{nb,n}\widehat{B}_{cp}\ddot{\widehat{\eta}}+\widehat{\omega}_{n,c.m}^{b}\times\widehat{R}_{nb,n}\widehat{M}_{fl}\left(\widehat{R}_{nb,n}\widehat{\omega}_{b,c.m}^{b}\right)\\&\quad+\left(\widehat{\omega}_{n,c.m}^{b}+\widehat{R}_{nb,n}\widehat{\omega}_{b,c.m}^{b}\right)\times\left(\widehat{R}_{nb,n}\widehat{M}_{fl}\widehat{\omega}_{n,c.m}^{b}+\widehat{R}_{nb,n}\widehat{B}_{cp}\dot{\widehat{\eta}}\right).\end{aligned} \tag{40}$$

Table 1: Orbital parameters of RFCS b.

Description	Parameters	Value
Eccentricity	e_b	0.02
Semimajor axis	a_b	6998455 m
Inclination	I_b	45°
Argument of perigee	ω_b	0°
Right ascension of the ascending node	Ω_b	0°
Initial true anomaly	f_b	30°

In addition, let

$$\begin{aligned}\widehat{M}_{b}=\widehat{M}_{fl}+\widehat{M}_{fr}&=\begin{bmatrix} [V_{fl}]_{v}^{\times} & m_{fl}I_{3\times3} \\ J_{fl} & [V_{fl}]^{\times} \end{bmatrix}+\begin{bmatrix} [V_{fr}]_{v}^{\times} & m_{fr}I_{3\times3} \\ J_{fr} & [V_{fr}]^{\times} \end{bmatrix}\\&=\begin{bmatrix} [V_{fl}]_{v}^{\times}+[V_{fr}]_{v}^{\times} & (m_{fl}+m_{fr})I_{3\times3} \\ J_{fl}+J_{fr} & [V_{fl}]^{\times}+[V_{fr}]^{\times} \end{bmatrix},\end{aligned} \tag{41}$$

where $J_b=J_{fl}+J_{fr}$ is the moment of inertia of RFCS b. $m_b=m_{fl}+m_{fr}$ is the mass of RFCS b.

In Equation (41), we can further obtain

$$\begin{aligned}[V_{fl}]_{v}^{\times}+[V_{fr}]_{v}^{\times}=0,\\ [V_{fl}]^{\times}+[V_{fr}]^{\times}=0.\end{aligned} \tag{42}$$

Introducing Equation (42) into Equation (41), the dual inertia operator of RFCS b can be expressed as

$$\widehat{M}_{b}=\begin{bmatrix} 0_{3\times3} & m_{b}I_{3\times3} \\ J_{b} & 0_{3\times3} \end{bmatrix}. \tag{43}$$

Substituting Equation (28) into Equation (40), the dynamics of the RFCS b with time-varying configuration can be obtained.

$$\begin{aligned}\widehat{F}_{b,n}^{b}&=\widehat{R}_{nb,n}\widehat{M}_{b}\left(\widehat{R}_{nb,n}\dot{\widehat{\omega}}_{b,c.m}^{b}\right)+\left(\widehat{R}_{nb,n}\widehat{\omega}_{b,c.m}^{b}\right)\\&\quad\times\widehat{R}_{nb,n}\widehat{M}_{b}\left(\widehat{R}_{nb,n}\widehat{\omega}_{b,c.m}^{b}\right)+\widehat{F}_{DR,n}^{b},\end{aligned}$$

$$\begin{aligned}\widehat{F}_{DR,n}^{b}&=\widehat{R}_{nb,n}\widehat{M}_{fl}\dot{\widehat{\omega}}_{n,c.m}^{b}+\widehat{R}_{nb,n}\widehat{B}_{cp}\ddot{\widehat{\eta}}+\widehat{\omega}_{n,c.m}^{b}\times\widehat{R}_{nb,n}\widehat{M}_{fl}\widehat{\omega}_{n,c.m}^{b}\\&\quad+\left(\widehat{\omega}_{n,c.m}^{b}+\widehat{R}_{nb,n}\widehat{\omega}_{b,c.m}^{b}\right)\times\widehat{R}_{nb,n}\widehat{B}_{cp}\dot{\widehat{\eta}},\end{aligned}$$

$$\widehat{F}_{DR,n}^{b}=\widehat{F}_{DE,n}^{b}+\widehat{F}_{CN,n}^{b}. \tag{44}$$

In Equation (44), the first equation represents the six-degree-of-freedom dynamics of the whole system; the second equation represents the relative motion between the flexible module and the FFSR. Equations in Equation (44) are equations of the RFCS with time-varying configuration,

Table 2: Characteristic parameters of RFCS b.

Description	Parameters	Value
Module mass	m_{fl}	20 kg
FFSR mass	m_{fr}	80 kg
Moment of inertia of the module	J_{fl}	$\begin{bmatrix} 40.34 & -4.92 & -8.50 \\ -4.92 & 207.05 & 29.93 \\ -8.50 & 29.93 & 233.33 \end{bmatrix}$ kg · m^2
Moment of inertia of FFSR	J_{fr}	diag {100, 150, 120}kg · m^2
Rigid-flex translational coupling matrix	B_{tran}	$[0.155 \quad -0.155 \quad 0.225]^T$
Rigid-flex rotational coupling matrix	B_{rot}	$[0.2 \quad 0.05 \quad 0.15]^T$
Modal damping ratio of the module	ξ	0.05
Stiffness of the module	Λ	1.727

which can also describe the 6 DOF motion of the spacecraft having rotational solar panels. The dynamic model of a satellite with rotational solar panels in Ref. [29] derived from the classical Newton-Euler method has the same form as Equation (44), which proves the correctness of the dynamic model proposed in this paper. Furthermore, Equation (44) is a general model which can describe the relative motion between two non-centroid points of spacecraft, while the classical Newton-Euler model cannot. In addition, the integrated relative dynamic equations of Equation (44) can improve the computational efficiency of the model.

In the rest of this section, an ideal physical scenario is assumed. In this scenario, the force exerted by the robot on the module, $\widehat{F}^b_{DE,n}$, is zero, and the module moves relative to the robot at a constant angular velocity, $\widehat{\omega}^b_{n,c.m}$. Ignore motion damping and other disturbances between the robot and the module. Then, in this scenario, the dynamics of the RFCS b with time-varying configuration can be expressed as

$$\begin{aligned}\widehat{F}^b_{b,n} &= \widehat{R}_{nb,n}\widehat{M}_b\left(\widehat{R}_{nb,n}\dot{\widehat{\omega}}^b_{b,c.m}\right) + \left(\widehat{R}_{nb,n}\widehat{\omega}^b_{b,c.m}\right) \\ &\times \widehat{R}_{nb,n}\widehat{M}_b\left(\widehat{R}_{nb,n}\widehat{\omega}^b_{b,c.m}\right) + \widehat{F}^b_{CN,n} = \widehat{R}_{nb,n}\widehat{M}_b\left(\widehat{R}_{nb,n}\dot{\widehat{\omega}}^b_{b,c.m}\right) \\ &+ \left(\widehat{R}_{nb,n}\widehat{\omega}^b_{b,c.m}\right) \times \widehat{R}_{nb,n}\widehat{M}_b\left(\widehat{R}_{nb,n}\widehat{\omega}^b_{b,c.m}\right) + \widehat{R}_{nb,n}\widehat{B}_{cp}\ddot{\widehat{\eta}} \\ &+ \widehat{\omega}^b_{n,c.m} \times \widehat{R}_{nb,n}\widehat{M}_{fl}\widehat{\omega}^b_{n,c.m} + \left(\widehat{\omega}^b_{n,c.m} + \widehat{R}_{nb,n}\widehat{\omega}^b_{b,c.m}\right) \times \widehat{R}_{nb,n}\widehat{B}_{cp}\dot{\widehat{\eta}}.\end{aligned} \tag{45}$$

In Equation (45), the variable quantity $\dot{\widehat{\eta}}$ is derived from η. According to Refs. [30, 31], η can be obtained through the following function:

$$\ddot{\eta} + 2\xi\Lambda\dot{\eta} + \Lambda^2\eta + B^T_{\text{tran}}\dot{v}^b_{s,n} + B^T_{\text{rot}}\dot{\omega}^b_{b,n} = 0, \tag{46}$$

where $\Lambda = \text{diag}\,[\Lambda_1 \quad \Lambda_2 \quad \cdots \quad \Lambda_N]$ is the natural frequency matrix of the flexible module, Λ_i is the ith natural frequency, ξ denotes the damping ratio of the flexible module, and $\mathbf{v}^b_{s,n}$ indicates the orbital velocity of RFCS b under the action of external forces, excluding gravity.

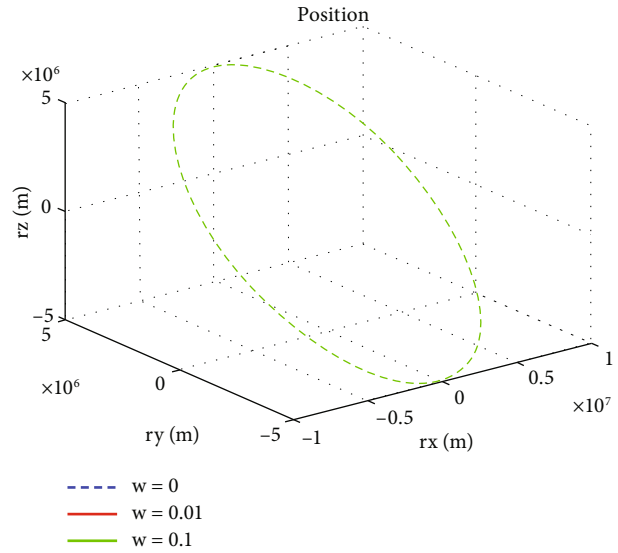

Figure 2: Orbit of RFCS.

4. Relative Dynamics between Two RFCS with Time-Varying Configuration

The relative motion state between RFCS b and RFCS a can be expressed as a dual quaternion.

$$\widehat{q}_{ba} = q_{ba} + \varepsilon\frac{1}{2}q_{ba}\tilde{r}^b_{ba,n}, \tag{47}$$

where $\widehat{q}_{ba} \in \mathbb{R}^{8\times1}$ denotes the relative dual quaternion state between two spacecrafts. $\tilde{r}^b_{ba,n} = \begin{bmatrix} 0 & r^b_{ba,n}{}^T \end{bmatrix}^T$; $r^b_{ba,n}$ denotes the relative position vector from o_b to o_a with respect to the body-fixed coordinate system of RFCS b. $q_{ba} \in \mathbb{R}^{4\times1}$ denotes the relative attitude quaternion.

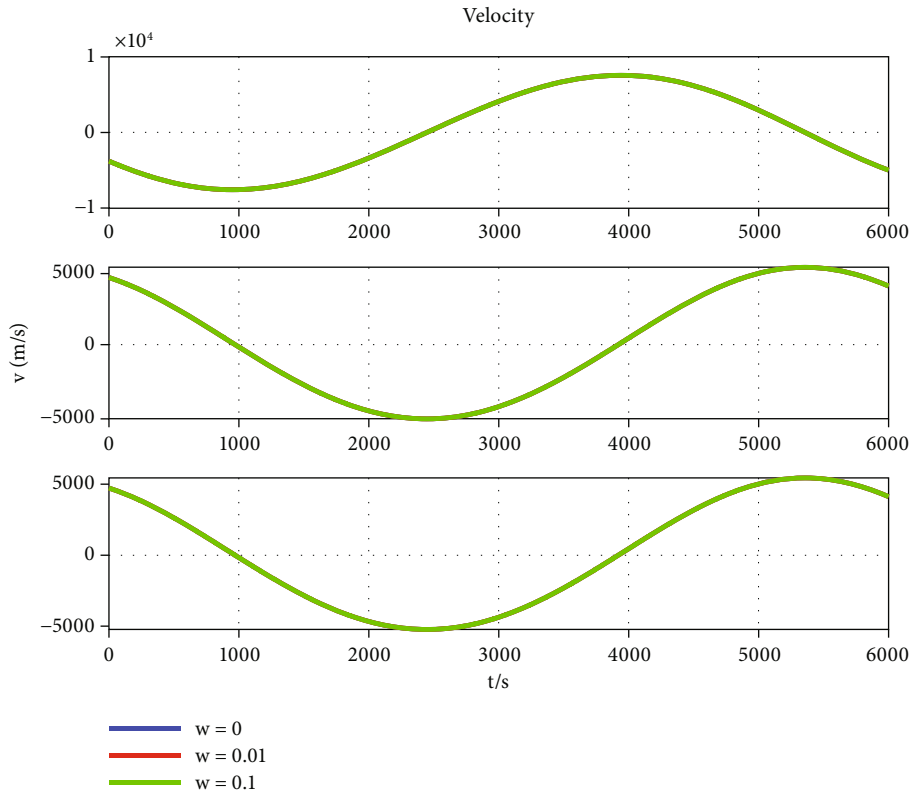

Figure 3: Velocity of RFCS under Case 1.

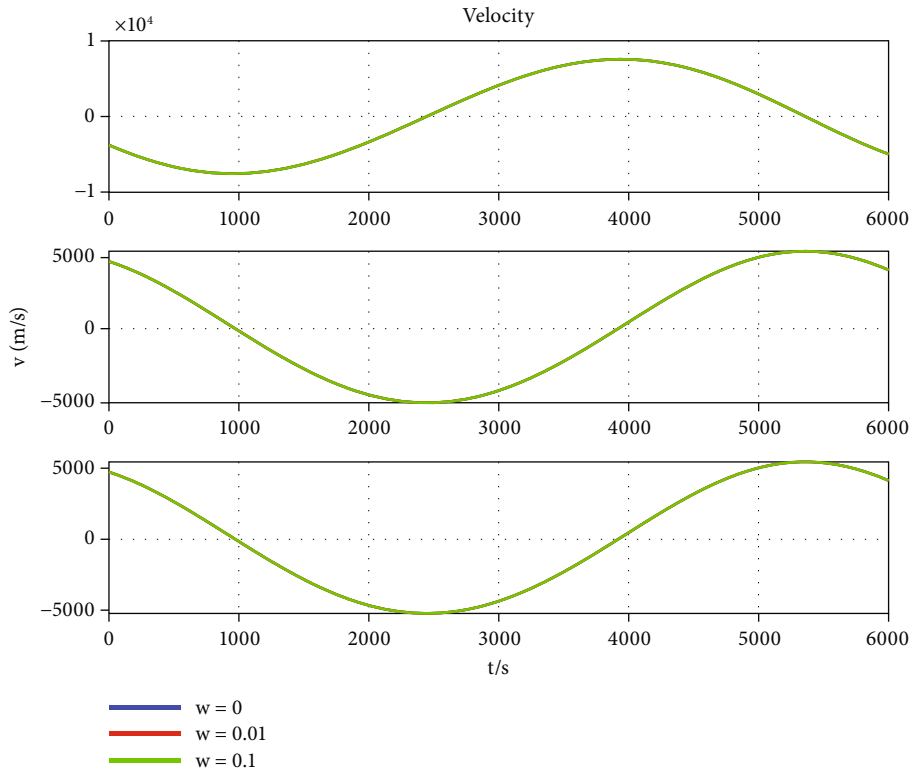

Figure 4: Position of RFCS under Case 1.

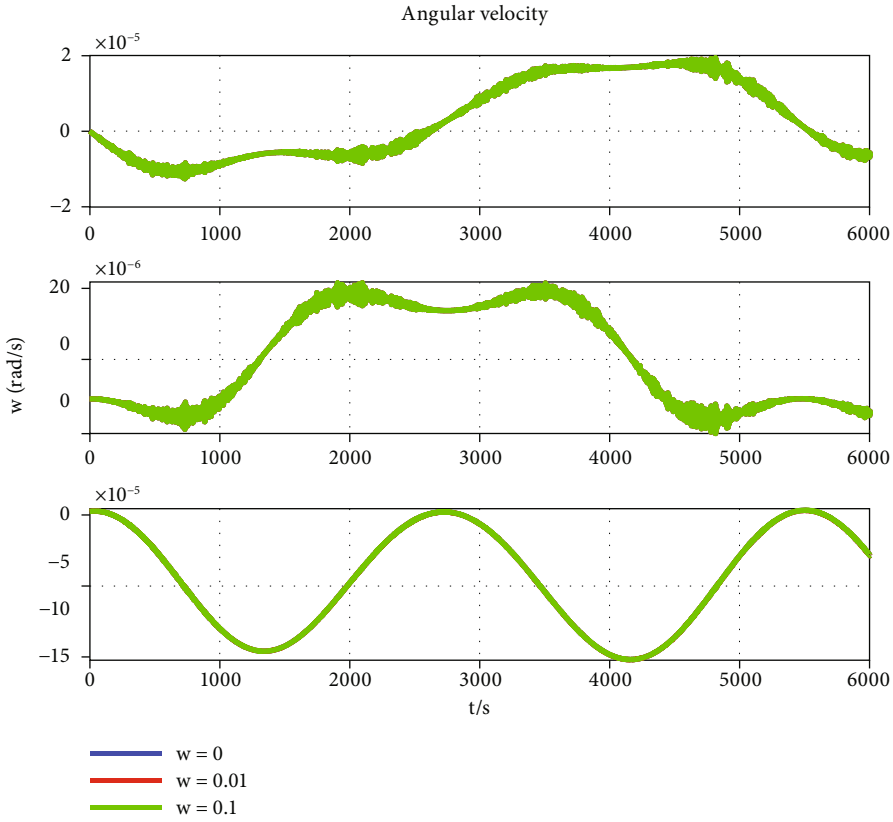

Figure 5: Angular velocity of RFCS under Case 1.

Furthermore, the relative kinematical equation can be represented as

$$\dot{\hat{q}}_{ba} = \frac{1}{2}\hat{q}_{ba}\tilde{\hat{\omega}}^{b}_{ba,n}, \tag{48}$$

where $\tilde{\hat{\omega}}^{b}_{ba,n} = [0 \quad \omega^{b}_{ba,n}{}^{T}]^{T} + \varepsilon[0 \quad v^{b}_{ba,n}{}^{T}]^{T}$; $\hat{\omega}^{b}_{ba,n} = \omega^{b}_{ba,n} + \varepsilon v^{b}_{ba,n}$. $v^{b}_{ba,n}$ is the relative orbital velocity and $\omega^{b}_{ba,n}$ is the relative angular velocity. $\hat{\omega}^{b}_{ba,n}$ is the relative dual velocity.

According to Ref. [21], $\hat{\omega}^{b}_{ba,n}$ can be derived from the following function:

$$\hat{\omega}^{b}_{ba,n} = \hat{\omega}^{b}_{b,c.m} - E_x\left\{\hat{q}^{*}_{ba}\tilde{\hat{\omega}}^{a}_{a}\hat{q}_{ba}\right\}, \tag{49}$$

where $\hat{\omega}^{a}_{a} = \omega^{a}_{a} + \varepsilon v^{a}_{a}$ and $\tilde{\hat{\omega}}^{a}_{a} = [0 \quad \omega^{a}_{a}{}^{T}]^{T} + \varepsilon[0 \quad v^{a}_{a}{}^{T}]^{T}$. v^{a}_{c} is the orbital velocity of RFCS a, $\boldsymbol{\omega}^{a}_{c}$ is the angular velocity of RFCS a, and the above two vectors are presented with respect to the body-fixed coordinate system of RFCS a. $E_x\{\cdot\}$ is the dimensionality reduction operator. The dimensionality reduction operator for an arbitrary eight-dimensional vector $\tilde{\hat{\omega}}^{a}_{a}$ is $E_x\{\tilde{\hat{\omega}}^{a}_{a}\} = \omega^{a}_{a} + \varepsilon v^{a}_{a}$.

According to Equation (49), the following equation can be obtained.

$$\begin{aligned}\dot{\hat{\omega}}^{b}_{ba,n} &= \dot{\hat{\omega}}^{b}_{b,c.m} - E_x\left\{\hat{q}^{*}_{ba}\tilde{\hat{\omega}}^{a}_{a}\hat{q}_{ba}\right\} \\ &= \dot{\hat{\omega}}^{b}_{b,c.m} - E^{-1}_{x}\left\{\hat{q}^{*}_{ba}\dot{\tilde{\hat{\omega}}}^{a}_{a}\hat{q}_{ba}\right\} + \hat{\omega}^{b}_{ba,n} \times E^{-1}_{x}\left\{\hat{q}^{*}_{ba}\tilde{\hat{\omega}}^{a}_{a}\hat{q}_{ba}\right\}.\end{aligned} \tag{50}$$

Substituting Equation (44) into Equation (50), the relative dynamics between RFCS b and RFCS a is obtained.

$$\begin{aligned}\dot{\hat{\omega}}^{b}_{ba,n} &= \hat{R}^{-1}_{nb,n}\hat{M}^{-1}_{b}\hat{R}^{-1}_{nb,n}\left(\hat{F}^{b}_{b,n} - \hat{F}^{b}_{DR,n}\right) - \hat{R}^{-1}_{nb,n}\hat{M}^{-1}_{b}\hat{R}^{-1}_{nb,n}\left(\hat{R}_{nb,n}\hat{\omega}^{b}_{b,c.m}\right) \\ &\quad \times \hat{R}_{nb,n}\hat{M}_{b}\left(\hat{R}_{nb,n}\hat{\omega}^{b}_{b,c.m}\right) - E^{-1}_{X}\left\{\hat{q}^{*}_{ba} \otimes E_X\left\{\dot{\hat{\omega}}^{a}_{a}\right\} \otimes \hat{q}_{ba}\right\} \\ &\quad + \hat{\omega}^{b}_{ba,n} \times E^{-1}_{X}\left\{\hat{q}^{*}_{ba} \otimes E_X\left\{\hat{\omega}^{a}_{a}\right\} \otimes \hat{q}_{ba}\right\} \\ &= \hat{R}^{-1}_{nb,n}\hat{M}^{-1}_{b}\hat{R}^{-1}_{nb,n}\hat{F}^{b}_{b,n} - \hat{R}^{-1}_{nb,n}\hat{M}^{-1}_{b}\hat{R}^{-1}_{nb,n}\left(\hat{R}_{nb,n}\hat{\omega}^{b}_{b,c.m}\right) \\ &\quad \times \hat{R}_{nb,n}\hat{M}_{b}\left(\hat{R}_{nb,n}\hat{\omega}^{b}_{b,c.m}\right) - \hat{R}^{-1}_{nb,n}\hat{M}^{-1}_{b}\hat{R}^{-1}_{nb,n} \\ &\quad \cdot \left[\hat{R}_{nb,n}\hat{M}_{fl}\dot{\hat{\omega}}^{b}_{n,c.m} + \hat{R}_{nb,n}\hat{B}_{cp}\ddot{\hat{\eta}} + \hat{\omega}^{b}_{n,c.m} \times \hat{R}_{nb,n}\hat{M}_{fl}\hat{\omega}^{b}_{n,c.m}\right. \\ &\quad \left. + \left(\hat{\omega}^{b}_{n,c.m} + \hat{R}_{nb,n}\hat{\omega}^{b}_{b,c.m}\right) \times \hat{R}_{nb,n}\hat{B}_{cp}\dot{\hat{\eta}}\right] \\ &\quad - E^{-1}_{X}\left\{\hat{q}^{*}_{ba} \otimes E_X\left\{\dot{\hat{\omega}}^{a}_{a}\right\} \otimes \hat{q}_{ba}\right\} + \hat{\omega}^{b}_{ba,n} \times E^{-1}_{X}\left\{\hat{q}^{*}_{ba} \otimes E_X\left\{\hat{\omega}^{a}_{a}\right\} \otimes \hat{q}_{ba}\right\}.\end{aligned} \tag{51}$$

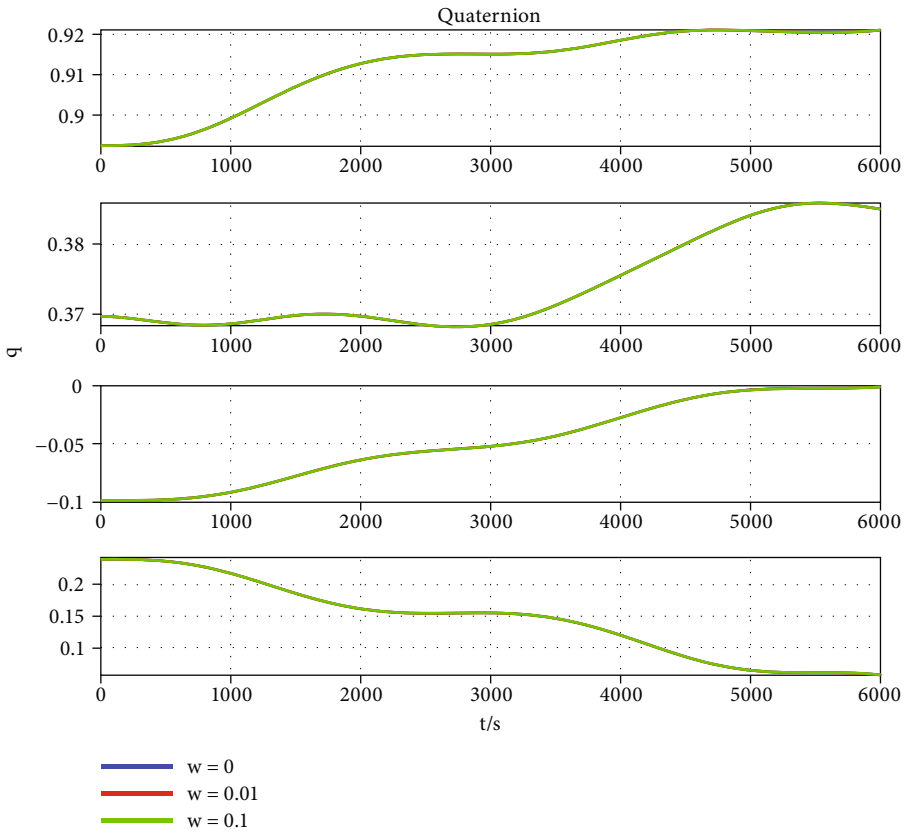

Figure 6: Attitude quaternion of RFCS under Case 1.

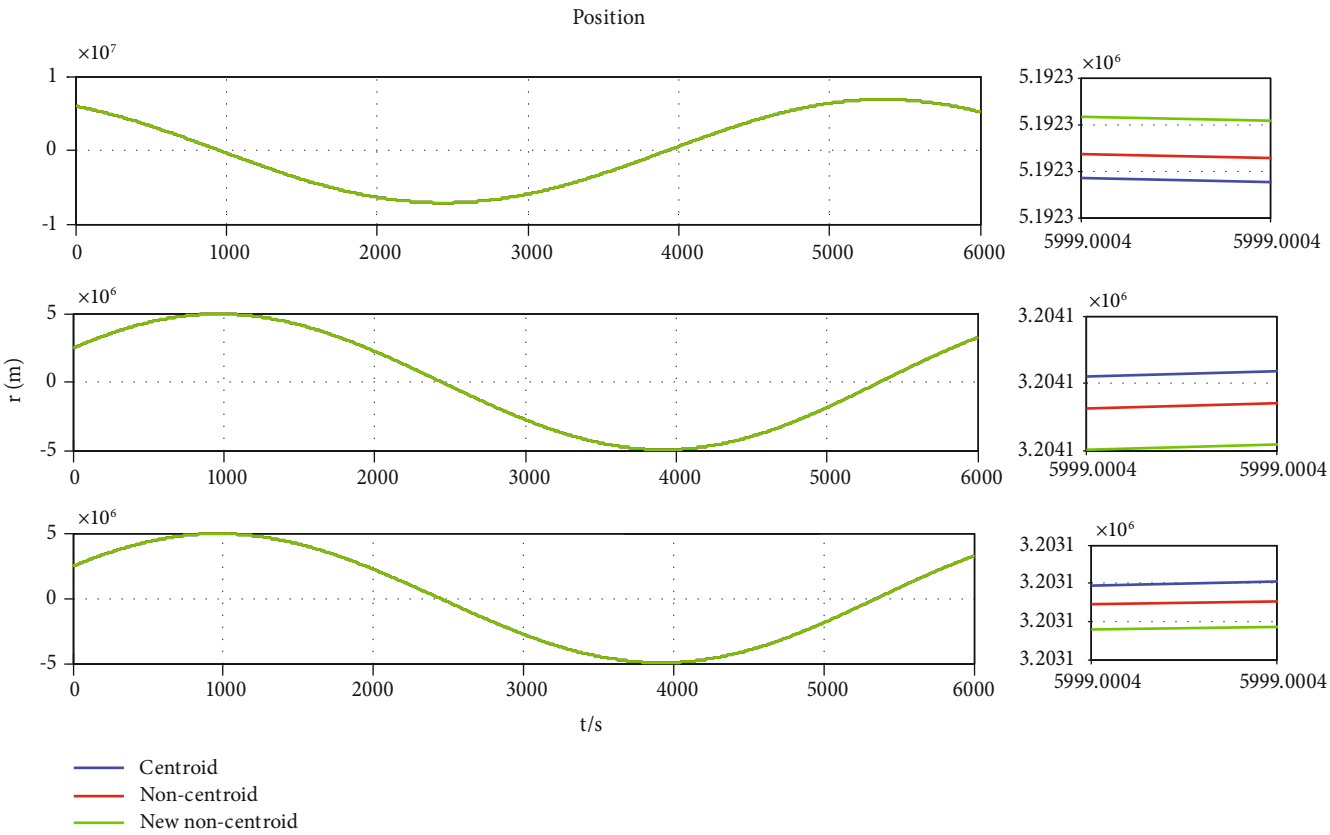

Figure 7: Position of RFCS under Case 2.

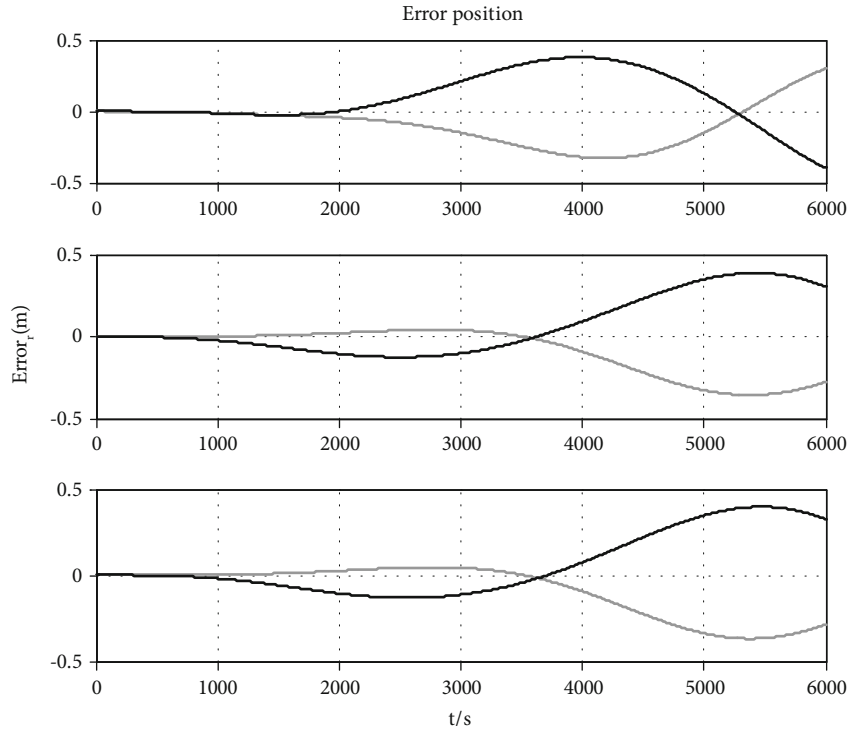

Figure 8: Error position of RFCS.

In the ideal physical scenario assumed in Section 3.3, if the force exerted by the robot on the module, $\widehat{F}^b_{DE,n}$, is zero, the relative dynamics equation can further be represented as

$$\begin{aligned}\dot{\widehat{\omega}}^b_{ba,n} &= \widehat{R}^{-1}_{nb,n}\widehat{M}^{-1}_b\widehat{R}^{-1}_{nb,n}\left(\widehat{F}^b_{b,n} - \widehat{F}^b_{CN,n}\right) - \widehat{R}^{-1}_{nb,n}\widehat{M}^{-1}_b\widehat{R}^{-1}_{nb,n}\left(\widehat{R}_{nb,n}\widehat{\omega}^b_{b,c.m}\right)\\ &\times \widehat{R}_{nb,n}\widehat{M}_b\left(\widehat{R}_{nb,n}\widehat{\omega}^b_{b,c.m}\right) - E^{-1}_X\left\{\widehat{q}^*_{ba}\otimes E_X\left\{\dot{\widehat{\omega}}^a_a\right\}\otimes\widehat{q}_{ba}\right\}\\ &+ \widehat{\omega}^b_{ba,n}\times E^{-1}_X\left\{\widehat{q}^*_{ba}\otimes E_X\left\{\widehat{\omega}^a_a\right\}\otimes\widehat{q}_{ba}\right\} = \widehat{R}^{-1}_{nb,n}\widehat{M}^{-1}_b\widehat{R}^{-1}_{nb,n}\widehat{F}^b_{b,n}\\ &- \widehat{R}^{-1}_{nb,n}\widehat{M}^{-1}_b\widehat{R}^{-1}_{nb,n}\left(\widehat{R}_{nb,n}\widehat{\omega}^b_{b,c.m}\right)\times\widehat{R}_{nb,n}\widehat{M}_b\left(\widehat{R}_{nb,n}\widehat{\omega}^b_{b,c.m}\right)\\ &- \widehat{R}^{-1}_{nb,n}\widehat{M}^{-1}_b\widehat{R}^{-1}_{nb,n}\left[\widehat{R}_{nb,n}\widehat{B}_{cp}\ddot{\widehat{\eta}} + \widehat{\omega}^b_{n,c.m}\times\widehat{R}_{nb,n}\widehat{M}_{fl}\widehat{\omega}^b_{n,c.m}\right.\\ &+ \left.\left(\widehat{\omega}^b_{n,c.m} + \widehat{R}_{nb,n}\widehat{\omega}^b_{b,c.m}\right)\times\widehat{R}_{nb,n}\widehat{B}_{cp}\dot{\widehat{\eta}}\right] - E^{-1}_X\left\{\widehat{q}^*_{ba}\otimes E_X\left\{\dot{\widehat{\omega}}^a_a\right\}\otimes\widehat{q}_{ba}\right\}\\ &+ \widehat{\omega}^b_{ba,n}\times E^{-1}_X\left\{\widehat{q}^*_{ba}\otimes E_X\left\{\widehat{\omega}^a_a\right\}\otimes\widehat{q}_{ba}\right\}.\end{aligned} \tag{52}$$

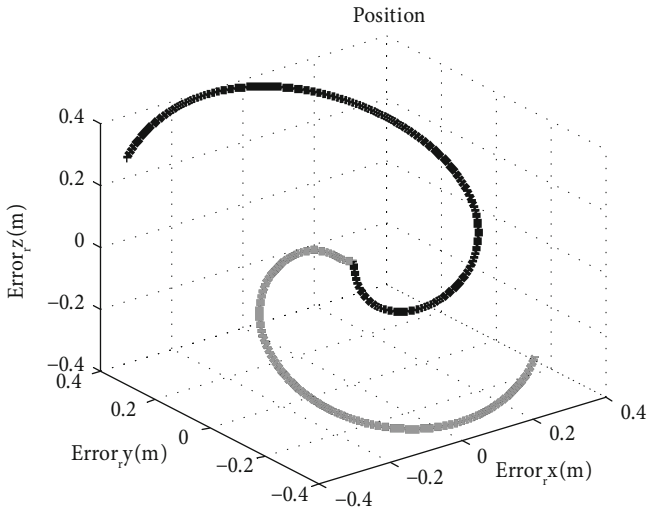

Figure 9: Error trajectory of RFCS.

5. Simulation Results

In this section, two sets of numerical simulations are provided. The first simulation was proposed to quantify the dynamics of RFCS with time-varying configuration in the ideal physical scenario assumed in Section 3.3 (Equation (45)). The influence of the relative attitude angular velocity, $\widehat{\omega}^b_{n,c.m}$, on the six-degree-of-freedom motion of the RFCS was analyzed. The second simulation was provided to analyze the influence of the coordinate origin selection of the BF coordinate system $o_b - x_b y_b z_b$ on relative motion description.

The initial position vector and orbit velocity of RFCS b with respect to the BF coordinate system $o_b - x_b y_b z_b$ are $r^b_{b,n}(0) = [6876550 \quad 0 \quad 0]^T$ m and $v^b_{b,c.m}(0) = [75.484 \quad 7679 \quad 0]^T$ m/s.

The initial attitude of RFCS b is set as $q_b(0) = [0.8924 \quad 0.3696 \quad -0.0990 \quad 0.2391]^T$ and $\omega^b_{b,c.m}(0) = [0 \quad 0 \quad 0]^T$ rad/s.

The dynamics equation (Equation (45)) is implemented in the case when the six-degree-of-freedom motion of RFCS b is governed by gravity

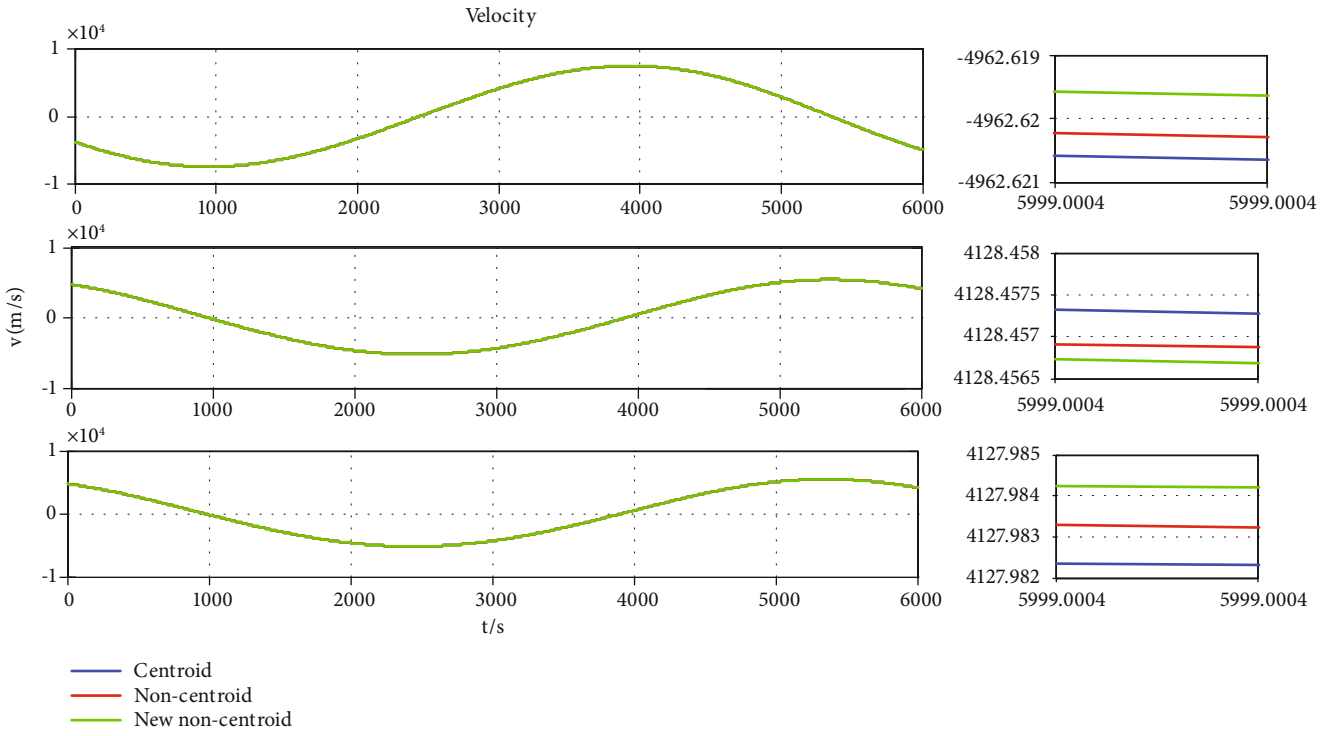

Figure 10: Velocity of RFCS under Case 2.

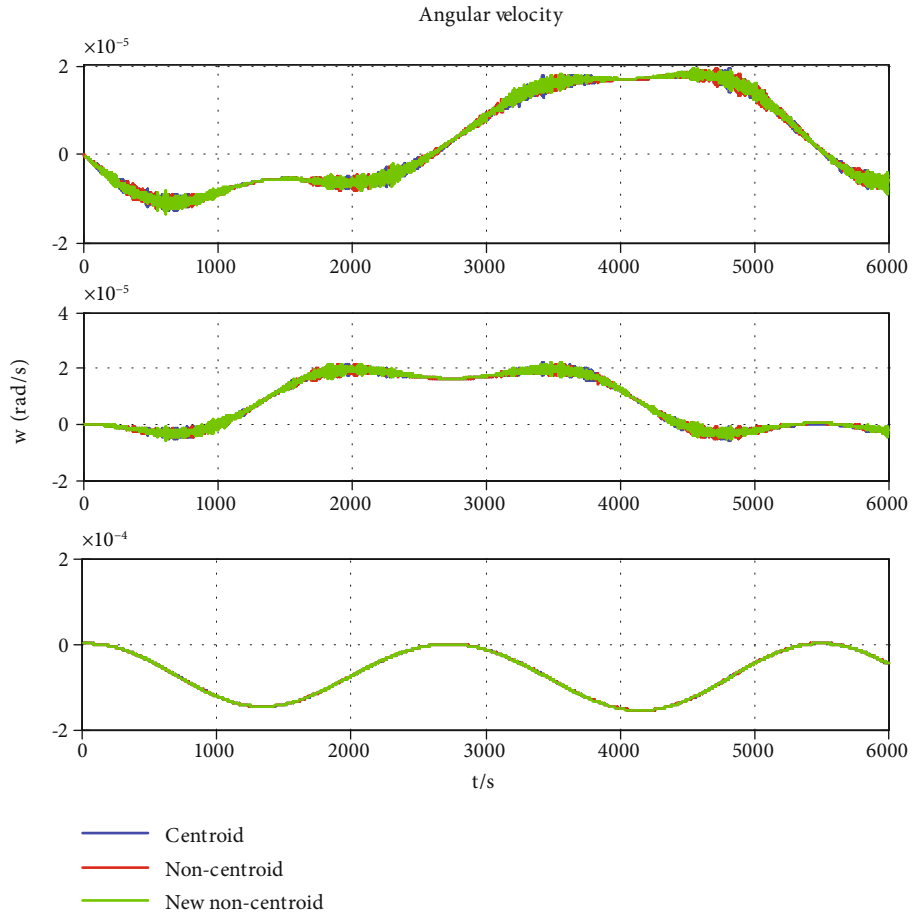

Figure 11: Angular velocity of RFCS under Case 2.

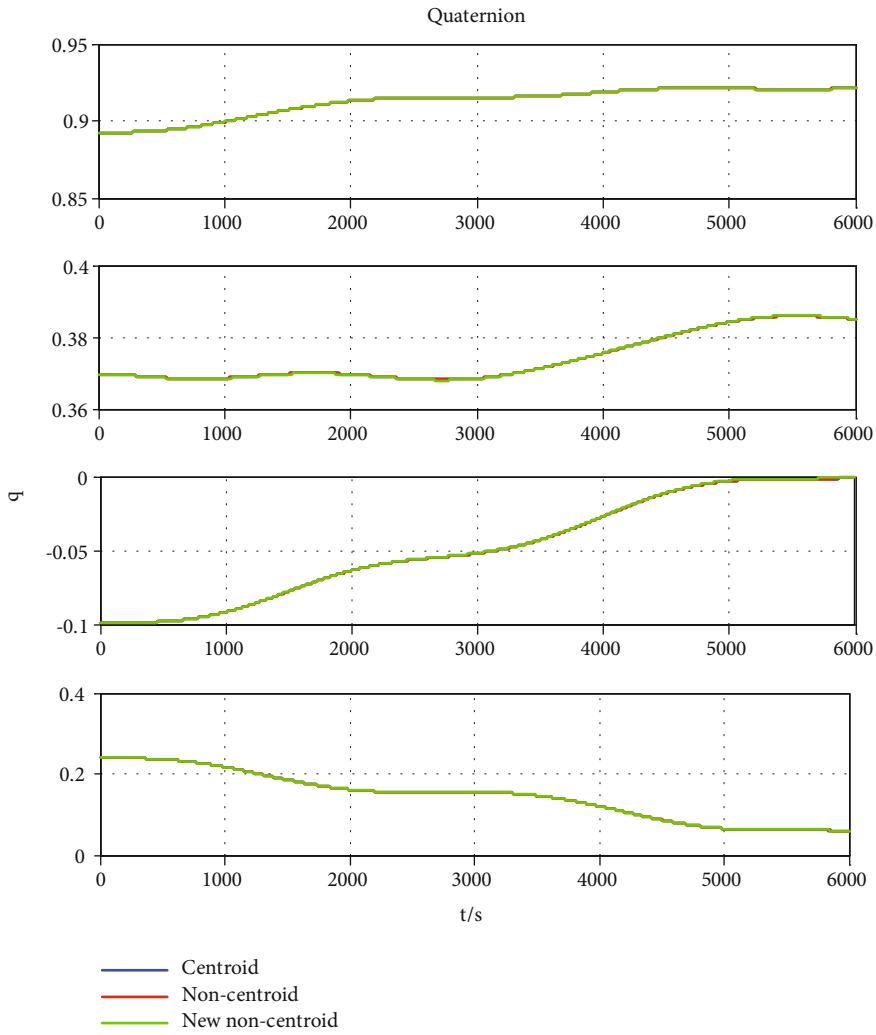

Figure 12: Attitude quaternion of RFCS under Case 2.

$(-\mu r^b_{b,n}/\|r^b_{b,n}\|^3, \mu = 398600.44\text{km}\cdot\text{s}^{-2})$ and the gravity gradient moment $(3\mu r^b_{b,n} \times Jr^b_{b,n}/\|r^b_{b,n}\|^5, \mu = 398600.44\text{km}\cdot\text{s}^{-2})$. The influence of other forces and noises are neglected. Table 1 lists the orbital parameters of RFCS b, and Table 2 lists the characteristic parameters of RFCS b.

5.1. Case 1: Effect of Relative Attitude Motion between the Flexible Module and FFSR on the Six-Degree-of-Freedom Motion of RFCS. Considering $r^a_{nb,n} = [-0.2 \quad -0.1 \quad 0.05]^T$ m, three sets of relative attitude angular, $\widehat{\omega}^b_{n,c.m} = [0 \quad 0 \quad 0]^T$, $\widehat{\omega}^b_{n,c.m} = [0 \quad 0 \quad 0.01]$rad/s, and $\widehat{\omega}^b_{n,c.m} = [0 \quad 0 \quad 0.1]$rad/s, were adopted, and the simulation results were obtained.

The blue lines, red lines, and green lines are the six-degree-of-freedom motion of RFCS when $\widehat{\omega}^b_{n,c.m} = [0 \quad 0 \quad 0]^T$, $\widehat{\omega}^b_{n,c.m} = [0 \quad 0 \quad 0.01]$rad/s, and $\widehat{\omega}^b_{n,c.m} = [0 \quad 0 \quad 0.1]$rad/s, respectively. Figure 2 shows the orbit of RFCS. Figures 3 and 4 show the orbit velocity and three-axis position of RFCS, respectively. Figures 5 and 6 show the angular velocity and attitude quaternion of the RFCS. As shown in Figures 2–6, in three cases, the six-degree-of-freedom motion curves of RFCS basically coincide. It shows that under the ideal condition assumed in Section 3.3, the relative rotational angular velocity between the module and FFSR has little effect on the six-degree-of-freedom motion of RFCS. The simulation results are consistent with the physical reality and prove the validity of the mathematical model for RFCS with time-varying configuration.

5.2. Case 2: Effect Coordinate Origin Selection of on the Description of the Six-Degree-of-Freedom Motion of RFCS. Considering $\widehat{\omega}^b_{n,c.m} = 0$, three sets of coordinate origin selection, $r^a_{nb,n} = [0 \quad 0 \quad 0]^T$m, $r^a_{nb,n} = [-0.2 \quad -0.1 \quad 0.05]^T$m, and $\widehat{R}_{nb,n} = [-0.5 \quad 0.3 \quad 0.2]^T$m, were adopted, and the simulation results were obtained:

In Figures 7–12, the blue lines represent the six-degree-of-freedom motion of RFCS when $r^a_{nb,n} = [0 \quad 0 \quad 0]^T$m. The red lines represent the six-degree-of-freedom motion of RFCS when $r^a_{nb,n} = [-0.2 \quad -0.1 \quad 0.05]^T$m. The green lines represent the six-degree-of-freedom motion of RFCS

when $\widehat{R}_{nb,n} = [-0.5 \quad 0.3 \quad 0.2]^T$m. The gray lines in Figures 8 and 9 represent the deviation curve between red and blue in Figure 7, and the black lines represent the deviation curve between green and red in Figure 7. As shown in Figures 11 and 12, the attitude angular velocity and attitude quaternion of RFCS do not change with the migration of the origin of the BF coordinate system. In Figures 7–10, as the distance between the origin of the BF coordinate system and the center of mass is larger, the position deviation of RFCS is larger. The positional deviation of the combined system reaches about 1 m when $\widehat{R}_{nb,n} = [-0.5 \quad 0.3 \quad 0.2]^T$m.

6. Conclusions

This paper proposed a dynamic model of rigid-flex combination systems with time-varying configuration. Dual quaternions were used to describe the six-dimensional spinor form of a rigid-flex combination system. The algebra of dual momentum for RFCS with time-varying configuration was developed, and the relative dynamics between two RFCSs with time-varying configuration for on-orbit assembly were provided. The simulation results show that the configuration changes have little effect on the six-degree-of-freedom motion of rigid-flex combination systems under the ideal physical scenario. The position error caused by the migration of the origin of the BF coordinate system is about 1 m. This shows that the selection of the origin of the BF coordinate system is key for the dynamic modeling of rigid-flex combination systems with time-varying configuration.

Data Availability

The data used to support the findings of this study are available from the corresponding author upon request.

Conflicts of Interest

The authors declare no conflicts of interest.

References

[1] L. Shi, X. Xiao, M. Shan, and X. Wang, "Force control of a space robot in on-orbit servicing operations," *Acta Astronautica*, vol. 193, pp. 469–482, 2022.

[2] Y. Ishijima, D. Tzeranis, and S. Dubowsky, "The on-orbit maneuvering of large space flexible structures by free-flying robots," in *The 8th International Symposium on Artifical Intelligence, Robotics and Automation in Space–ISAIRA*, Munich, Germany, 2005.

[3] E. Uzo-Okoro, P. Manandhar, D. Erkel, M. Dahl, and O. Weck, "Optimization of on-orbit robot assembly of small satellites," in *ASCEND 2020*, Las Vegas, USA, 2020.

[4] S. Moosavian and E. Papadopoulos, "Free-flying robots in space: an overview of dynamics modeling, planning and control," *Robotica*, vol. 25, no. 5, pp. 537–547, 2007.

[5] K. Shi, C. Liu, Z. Sun, and X. Yue, "Coupled orbit-attitude dynamics and trajectory tracking control for spacecraft electromagnetic docking," *Applied Mathematical Modelling*, vol. 101, pp. 553–572, 2022.

[6] B. Lyu, C. Liu, and X. Yue, "Hybrid nonfragile intermediate observer-based T-S fuzzy attitude control for flexible spacecraft with input saturation," *Aerospace Science and Technology*, vol. 128, article 107753, 2022.

[7] F. Yohsuke, I. Noriyasu, and O. Mitsushige, "Capture and berthing experiment of a massive object using ETS7 space robot," in *AIAA Astrodynamics Specialist Conference*, Denver, USA, 2000.

[8] S. Dubowsky and P. Boning, "Coordinated control of space robot teams for the on-orbit construction of large flexible space structures," *Advanced Robotics*, vol. 24, no. 3, pp. 303–323, 2010.

[9] D. Woffinden and D. Geller, "Navigating the road to autonomous orbital rendezvous," *Journal of Spacecraft and Rockets*, vol. 44, no. 4, pp. 898–909, 2007.

[10] X. Liu, H. Li, Y. Chen, G. Cai, and X. Wang, "Dynamics and control of capture of a floating rigid body by a spacecraft robotic arm," *Multibody System Dynamics*, vol. 33, no. 3, pp. 315–332, 2015.

[11] X. Cyril, A. Misra, M. Ingham, and G. Jaar, "Postcapture dynamics of a spacecraft-manipulator-payload system," *Journal of Guidance, Control and Dynamics*, vol. 23, no. 1, pp. 95–100, 2000.

[12] T. Chau, N. Huynh, and I. Sharf, "Capture of spinning target with space manipulator using magneto rheological damper," in *AIAA Guidance, Navigation, and Control Conference*, Toronto, Canada, 2010.

[13] H. Gao, G. Ma, Y. Lv, and Y. Guo, "Forecasting-based data-driven model-free adaptive sliding mode attitude control of combined spacecraft," *Aerospace Science and Technology*, vol. 86, pp. 364–374, 2019.

[14] H. Gao, G. Ma, Y. Lv, and Y. Guo, "Data-driven model-free adaptive attitude control of partially constrained combined spacecraft with external disturbances and input saturation," *Chinese Journal of Aeronautics*, vol. 32, no. 5, pp. 1281–1293, 2019.

[15] B. Lyu, X. Yue, and C. Liu, "Constrainedmulti-observer-based fault-tolerant disturbance-rejectioncontrol for rigid spacecraft," *International Journal of Robust and Nonlinear Control*, vol. 32, no. 14, pp. 8102–8133, 2022.

[16] C. Liu, X. Yue, J. Zhang, and K. Shi, "Active disturbance rejection control for delayed electromagnetic docking of spacecraft in elliptical orbits," *IEEE Transactions on Aerospace and Electronic Systems*, vol. 58, no. 3, pp. 2257–2268, 2021.

[17] K. Li, Q. Tian, J. Shi, and D. Liu, "Assembly dynamics of a large space modular satellite antenna," *Acta Astronautica*, vol. 142, article 103601, 2019.

[18] V. Kapila, A. Sparks, J. Buffington, and Q. Yan, "Spacecraft formation flying: dynamics and control," *Journal of Guidance, Control and Dynamics*, vol. 23, no. 3, pp. 561–564, 2000.

[19] W. Clohessy and R. Wiltshire, "Terminal guidance system for satellite rendezvous," *Journal of the Aerospace Sciences*, vol. 27, no. 9, pp. 653–658, 1960.

[20] V. Brodsky and M. Shoham, "Dual numbers representation of rigid body dynamics," *Mechanism and Machine Theory*, vol. 34, no. 5, pp. 693–718, 1999.

[21] B. Qiao, S. Tang, K. Ma, and Z. Liu, "Relative position and attitude estimation of spacecrafts based on dual quaternion for rendezvous and docking," *Acta Astronautica*, vol. 91, pp. 237–244, 2013.

[22] T. Chen, H. Hu, and D. Jin, "On-orbit assembly of a team of flexible spacecraft using potential field based method," *Acta Astronautica*, vol. 133, pp. 221–232, 2017.

[23] J. Sun, X. Zhang, X. Wu, and T. Song, "Dual-quaternion-based translation-rotation-vibration integrated dynamics modeling for flexible spacecraft," *Journal of Aerospace Engineering*, vol. 32, no. 1, article 04018135, 2019.

[24] X. Zhang, W. Zhu, X. Wu, T. Song, Y. Xie, and H. Zhao, "Dynamics and control for in-space assembly robots with large translational and rotational maneuvers," *Acta Astronautica*, vol. 174, pp. 166–179, 2020.

[25] X. Zhang, W. Zhu, Y. Xie, X. Wu, and J. Guo, "Cross-coupling relative dynamics for on-orbit assembly in rotating frame of reference," *Applied Mathematical Modelling*, vol. 116, pp. 372–392, 2023.

[26] P. Likins, "Modal method for analysis of free rotations of spacecraft," *AIAA Journal*, vol. 5, no. 7, pp. 1304–1308, 1967.

[27] P. Likins and P. Wirsching, "Use of synthetic modes in hybrid coordinate dynamic analysis," *AIAA Journal*, vol. 6, no. 10, pp. 1867–1872, 1968.

[28] Q. Yuan, Y. Liu, and N. Qi, "Active vibration suppression for maneuvering spacecraft with high flexible appendages," *Acta Astronautica*, vol. 139, no. 10, pp. 512–520, 2017.

[29] W. Hooker, "A set of r dynamical attitude equations for an arbitrary n-body satellite having r rotational degrees of freedom," *AIAA Journal*, vol. 8, no. 7, pp. 1205–1207, 1970.

[30] Y. Yan and B. Yue, "Dynamic analysis of the flexible spacecraft with liquid sloshing in axisymmetrical container," *Journal of Spacecraft and Rockets*, vol. 55, no. 2, pp. 282–291, 2018.

[31] C. Sun, Y. Xiao, Z. Sun, and D. Ye, "Dual quaternion based close proximity operation for in-orbit assembly via model predictive control," *International Journal of Aerospace Engineering*, vol. 2021, Article ID 1305095, 14 pages, 2021.